Research Article

Phosphorus and sulphates removal from wastewater using copper smelter slag washed with acid

Moatlhodi Wise Letshwenyo[1] (ID) · **Gobusaone Mokokwe**[1]

© The Author(s) 2021   OPEN

Abstract

In this study, we present the performance of acid washed copper smelter slag for the adsorption of phosphates and sulphates from wastewater. The aim of the study was to investigate the removal of phosphates and sulphates from wastewater using acid washed copper smelter slag at batch scale by exploring influences of different variables. The leachate concentrations of copper, iron, manganese and lead released from the adsorbent were 1.8, 128.2, 0.32 and 0.20 mg L^{-1}, respectively at pH 2. The point of zero charge was at pH 6.04, Pseudo-Second Order kinetic model described the adsorption process better with an R^2 value of 0.99. The experimental maximum adsorption capacities for phosphates and sulphates were 0.51 and 0.24 mg g^{-1} media, respectively, and 0.96 mg P g^{-1} media at pH 12 and 0.39 mg g^{-1} media for sulphates at pH 2, respectively. The process was endothermic with temperature having insignificant impact during adsorption. The maximum adsorption capacities for thermodynamic study were 0.103 ± 0.09 and 0.046 ± 0.004 mg g^{-1} media respectively, for PO_4^{3-} P and SO_4^{2-} at 60 °C. This study showed that acid washed copper smelter slag has an improved adsorption capacity for phosphate and sulphate ions but further investigations should be conducted to find ways of further improving the adsorbent performance.

Article highlights

- There is increase in the adsorption capacity of acid washed copper smelter slag.
- The adsorption capacity of phosphorus is high at pH 12 and for sulphate at pH 6.
- The adsorption of phosphate and sulphate ions onto acid washed slag is an endothermic process.
- Intraparticle diffusion was not the only rate controlling mechanisms.

1 Introduction

The presence of phosphorus in wastewater effluent discharges promotes eutrophication in water bodies even at concentrations as low as 0.02 mg L^{-1} [1]. The presence of sulphates and phosphates in surface water reservoirs such as rivers is the result of discharges from sewage and from agricultural activities and runoffs in the case of phosphates [2]. Other sources of phosphate are waters that contain detergents in the solution from ingredients

---

which contributing to eutrophication [2]. Conventional technologies such as biological treatment and chemical precipitation are disadvantaged by high technical requirements, a high carbon foot print and high economic costs [3]. Biological phosphorus removal systems limit the recovery of the nutrient from the sludge, resulting in wasteful use [4]. Some studies have revealed that the conventional technologies have a high carbon foot print resulting in the emissions of greenhouse gases which include carbon dioxide, methane and nitrogen oxides leading to global warming and climate change [5], this is also reported by Campos et al. [6]. Adsorption technology has been perceived as a better option compared to the other technologies because adsorbents can be regenerated and therefore reused before being replaced with new media hence reducing the costs [7]. Sludge is not generated, which reduces the handling, transportation and disposal costs. In addition, efficiency and low costs are among the benefits of the technology over conventional methods [7]. Other technologies like chemical precipitation produce toxic sludge that restricts reuse and also poses a risk to the environment. In their study, Kumar et al. [8] highlighted that the expenses related to chemical costs for lowering phosphate concentration from 10 to 1 mg P L^{-1} was \$ 8 kg^{-1} P when using chemical precipitation technology. This is compared to \$ 35 kg^{-1} P for the chemical costs when adsorption technology is used. However, it was observed that since the concentration of phosphate ion was low, the cost of adsorption is better than that of precipitation, indicating that adsorption is better suited for low concentrated wastewaters. Coagulation or flocculation has the disadvantage of increased sludge production which increases management, and treatment costs because flotation technology requires high initial capital costs and high energy costs [9].

Sulphates are the major pollutants of groundwater and at concentrations exceeding 250 mg L^{-1}, can cause a bad taste in the water, corrode water pipes and lead to some discomforts in human beings such as laxative effects and gastrointestinal irritation [10]. This implies that discharges of wastewater effluents containing sulphates exceeding threshold values can be found in the environment, groundwater and surface water, and they pose contamination risk. Conventional technologies for treating wastewaters containing sulphates for instance membrane filtration, biological treatment, chemical precipitation and many more are not suitable for the removal of sulphates at high concentrations[11], hence the need to explore different technologies. Adsorption technology has been studied before. For example [12] investigated the removal of sulphates from wastewater using natural alum inosilicate modified with uric acid. It was observed that 60% of the initial 500 mg L^{-1} concentration was eliminated

from the solution, which indicated that the process has some promising results.

Different materials have been investigated as adsorbents for phosphorus from wastewater [13–15]. Some of the investigations were carried out on industrial waste such as drinking water treatment sludge [16], synthetic materials such as magnetic iron oxide nanoparticles [17], activated aluminum oxide and lanthanum oxide [18]. Some materials have been modified, treated and even examined by varying experimental conditions. The modifications and the alterations of experimental conditions are aimed at enhancing the adsorption capacities. Table 1 below illustrates some of the modifications and treatments subjected to media for capacity improvement.

Excessive sulphates (SO_4^{2-}) concentrations cause a natural imbalance in the sulphur cycle and pose a risk to public health, but in countries there are no set guidelines due to lower toxicity of SO_4^{2-} [27]. A study by Wei et al. [28] observed a reduction in the retention capacity for sulphate when the adsorbent dose was increased when using organo-nano- clay as the adsorbent. It has also been observed that increasing contact time and temperature increased the adsorption capacity of the material. A similar study by Sadik et al. [29] reported that the adsorption equilibrium for sulphate on mixed oxide LDH was reached after 60 min, which indicates that the process was very fast.

Many studies have not investigated the uptake of both phosphate and sulphate ions from real wastewater, except using synthetic solutions that lack the background concentrations of the different variables present in wastewater. These can have negative effects such as competition with the targeted pollutants, therefore reducing their uptakes. The presence of anions in wastewater such as nitrates (NO_3^-), fluorides and chlorides, can have competing effects with the targeted adsorbates. However, there are instances where the adsorbent has no affinity for anions as [30] observed that NO_3^- even in high concentrations such as 100 mg L^{-1} showed less competition with other anions for adsorption. Recently, dams have been built in many rivers in the area for water abstraction for potable use. Therefore, a controlled discharge of nutrient enriched wastewaters into surface water bodies is necessary, otherwise algal bloom will become a problem. If nutrients, including phosphorus, which is the limiting nutrient, are discharged into streams, algal bloom is likely to occur, which degrade the quality of stream water and increase the cost of stream water treatment [31].

The copper smelter slag that was used in the study was sourced from a neighbouring town where copper and nickel are produced. The slag had been stockpiled as a waste materials and is abundant in millions of tons at the mining site and has not been used. Furthermore,

Table 1 Modifications and treatments subjected to some of the adsorbents to enhance performance

Media	Preparation/modification	Target pollutant	Adsorption capacity (mg g^{-1})	References
Calcium-flour biochar	Carbonization at 800 °C in tube furnace. Heated at 10 °C/min to 600 °C in N_2 presence holding for 2 h	Phosphates	314.22	[19]
Thermally modified copper tailings	Heated for 2 h at 340 °C in muffle furnace	Phosphates	Adsorption capacity improved from 2.08 to 14.25 after treatment	[20]
Sulphate coated zeolite (SCZ)	Zeolite was coated with sulphate onto the surfaces through a redox process	Phosphates	111.49	[21]
Immobilization of powdery calcium silicate hydrate	PVA cross-linking reaction	Phosphates	31.06	[22]
Surfactant-Modified Palygorskite	10 g of palygorskite, ground to colloidal size and placed into 250 mL flask. 2 mol/kg hydrochloric acid added. Mixture refluxed for 2 h at 343 K	Sulphates	3.28	[23]
Modified steel slag and cement	Milled slag mixed with quartz sand, cement and permeable bricks	phosphates	1.06 to 18.88	[24]
Modified Biopolymer Adsorbents	Chitosan pellets in a glutaraldehyde (GA) solution were soaked at pH 5.6 for 48 h	Sulphates	46.6	[25]
Magnetic multi-walled carbon nanotubes (MWCNTs)	The MWCNTs dispersed in concentrated sulfuric acid and concentrated nitric acid (a 3:1 volume ratio) to modify the MWCNTs surface by ultrasonication for 4 h	Sulphates	93.28% efficiency	[26]

the disposal of the material will cost some millions of Botswana Pula. Recently, studies have been conducted on the possible uses of the slag, such as for the adsorption of heavy metals from wastewater or aqueous solutions, and the possibility of using the material for brick moulding. The possibility of slag being successful in the adsorption of phosphate and sulphate ions will be an added advantage for the use of the waste material. There is also a need to prevent eutrophication of surface waters, which can be caused by the discharge of phosphorus into the environment. The aim of this study was to examine acid washed copper smelter slag, a waste material from mining activities, as an adsorbent for phosphorus and sulphates from wastewater at batch scale mode. The key objectives were:

(a) To investigate the leachability of heavy metals from the media for possible environmental pollution.
(b) To investigate the impact of contact time and the rate controlling mechanisms during the adsorption process.
(c) To investigate the effect of media dosage during the adsorption process.
(d) To investigate the influence of initial pH during the adsorption process.

(e) To investigate the influence of temperature and thermodynamics during the adsorption process.

This study was conducted to test the hypothesis that acid washed copper smelter slag performed better than previously used unwashed slag in removing phosphates and sulphates from wastewater.

This research presents the findings of laboratory batch studies on the investigation of the removal of phosphates and sulphates from wastewater sing acid washed copper smelter slag. Different variables were investigated for their influence on the adsorbent performance. These include among others pH, temperature, contact time and media dosage impacts. The results of the study will help in deciding whether the material can be of better use at a field scale for the treatment of secondary wastewater effluent or any further investigations. The experimental procedure is discussed under materials and methods which includes adsorbent characterisation, adsorbate to be treated, determination of point of zero charge the pH leachability test, kinetic studies, media dosage and isotherms, effect of initial pH, thermodynamics. The section is followed by the results and discussion section, the practical implications and lastly the conclusion of the study.

2 Materials and methods

2.1 Adsorbent characterization

A study by Letshwenyo and Sima [32] investigated the possibility of using the raw copper smelter slag for phosphorus removal from real wastewater. In this study, the same material was washed with a 2.0 M hydrochloric acid (HCl) solution and investigated for the removal of PO_4^{3-} P and SO_4^{2-} from secondary treated wastewater. The material was sourced from BCL LTD, where it is stockpiled as waste.

For the preparation of the adsorbent, the slag was first crushed to reduce the sizes and then passed or sieved through the 4.75 mm and 1.18 mm sieve openings and the material retained on the 1.18 mm sieve was used for the investigation. A solid/liquid ratio of 20 mL g^{-1} as per Huang et al. [3] protocol was adopted. The mixture was placed into a 1000 mL beaker, stirred continuously for 10 min, and then agitated at 120 rpm for 24 h. The mixture was placed onto the 1.18 mm sieve to filter the acid. The residue was rinsed twice with deionised (DI) water and dried for one week at room temperature (25 °C). Washing the slag with HCl aimed to remove the residual phosphorus attached to calcium [33], as this could improve the adsorption capacity of the copper smelter slag.

The adsorbent surface morphology was investigated by scanning electron microscopy (SEM), Gemini 500, FGSEM, manufactured by Perkin Elmer model GEMINI 500, Serial number, Gemini Sem 00-70-18, P00225, using SmartSem software, Version 5.09 April 2015. The chemical composition was determined using X-Ray Fluorescence (Delta Professional).

The bulk density (ρ_b), particle density (ρ_p) and porosity (n) were evaluated as per the procedure described by Dan—Asabe et al. [34]. The following protocol was followed to determine the bulk density in g cm^{-3}, and the particle density (ρ_p), in g cm^{-3}. A 50 g of the prepared slag was placed in a 100 mL measuring cylinder. The cylinder was gently tapped to stabilise the slag and reading off the volume occupied by the slag. The study was conducted in triplicates and the mean volume was calculated. The bulk density was calculated as per [35]:

$$\rho_b = \frac{\text{mass of sludge (g)}}{\text{Volume of sludge (mL)}} \qquad (1)$$

The density of the particle (ρ_p) was calculated as per as per [35]:

$$\rho_p = \frac{\text{mass of sludge (g)}}{\text{volume of sludge (mL)}} \qquad (2)$$

The porosity (n) was calculated from the equation as per [36]:

$$n = \left(1 - \frac{\rho_b}{\rho_p}\right) \times 100 \qquad (3)$$

2.2 Adsorbates

The wastewater effluent used during this study was collected from the final maturation pond outlet of wastewater treatment facility in the study area and the collection were collected in the mornings. The PO_4^{3-} P concentration of the effluent used throughout the study varied between 21.4 and 25. 2 mg P L^{-1} and SO_4^{2-} concentration varied between 13.64 and 16.73 mg SO_4^{2-} L^{-1}. The concentrations of the other anions that could compete with PO_4^{3-} P and SO_4^{2-} for adsorption are in Table 2. As observed, nitrates, nitrite and phosphates exceeded the national threshold. The wastewater was passed through a 0.45 μm Whatman filter paper to retain solids. The ionic strengths or concentrations of each ion were determined using Ion Chromatography, of model ICS 500 + maker Dionex supplied by Thermo Scientific.

2.3 The zero point of charge

The protocol previously described by Letshwenyo and Mokgosi [36] was adopted to determine the point of zero charge of the adsorbent, in which 0.5844 g of sodium chloride (NaCl) was dissolved into 1 L of deionised (DI) water for the preparation of a 0.01 M solution of NaCl. This was followed by placing 50 mL of the prepared solution into eight different 250 mL Erlenmeyer flasks, in triplicates as per the protocol described by Letshwenyo and Mokgosi [36]. Hydrochloric (HCl) acid and sodium hydroxide (NaOH) solutions used to adjust the pH and

Table 2 The physiochemical parameters of wastewater used in this study

Parameter	Concentration (mg L^{-1})	National thresholds (mg L^{-1})
pH	7.46	6.5–9.0
Fluoride	0.17	1.5
Chloride	74.78	600
Bromide	0.0	Not stated
Nitrates	189.91	50
Nitrite	59.44	3
Sulphates	16.73	400
Phosphates	25.2	1.5
Turbidity (NTU)	43	30
Total suspended solids	45	25
Biochemical oxygen demand	41	30
Chemical oxygen demand	83	150

the working pH were between 2 and 12. A 5.0 g of acid washed copper smelter slag was added to each flask, with the exception of one flask which was a control [36]. The flasks were then agitated at 120 rpm for 48 h on the orbital shaker. The flasks were removed from the shaker up on reaching the pre-set time, and the mixtures was filtered through a 0.45 µm Whatman paper to separate the solids from the liquid. The average pH of each filtrate was then determined. The point of zero charge was determined as per [37] protocol.

2.4 The pH leachability test

The pH leachability test was conducted according to the description by Krol et al. [38]. This was achieved by adding 100 mL of DI water into a 250 mL Erlenmeyer flask. The pH was adjusted to the pH range of 2 and 12 using either nitric acid (HNO_3) or sodium hydroxide (NaOH) as described by Letshwenyo and Mokgosi [36]. Next, 2.0 g of the adsorbent was added in triplicates into each flask. The mixtures were shaken on the orbital shaker for 2 days at agitation speed of 120 rpm. Upon reaching the time, the flasks were removed from the shaker and the mixtures filtered through 0.45 µm Whatman filter papers as previously described [36]. The concentrations of the metal ions in the solution were measured and averages calculated using the inductively coupled plasma optical emission spectrometer, Thermo iCAP supplied by Thermo Scientific, from the United Kingdom.

2.5 Kinetic studies

In order to determine the optimum contact time and controlling mechanisms of adsorption processes such as mass transfer and chemical reactions, 2.0 g of adsorbent and 100 mL of wastewater were added into the flasks as described by Letina and Letshwenyo [35]. The flasks were agitated on the orbital shaker at 120 rpm and removed at different time intervals (10–240 min). The mixtures were filtered in the same way as previously described [36] and the concentrations of PO_4^{3-} P and SO_4^{2-} were measured in the filtrate. It was observed that an increase in the optimum contact time did not result in any PO_4^{3-} P and SO_4^{2-} removal. The experimental data were then fitted onto the widely published kinetic models of Pseudo-First Order (PFO), Pseudo-Second Order (PSO) and Intraparticle Diffusion Models. The kinetic equations and the meanings of the relevant coefficients are as described by Jellali et al. [39] and Wei et al. [40]. The amount of adsorbed PO_4^{3-} P and SO_4^{2-} at any particular time was calculated from the following equations described by Wei et al. [40]:

$$q_t = \frac{(C_0 - Ct)}{M}V \qquad (4)$$

where q_t (mg g^{-1} media), C_o (mg L^{-1}), C_t (mg L^{-1}) are the adsorption capacity at equilibrium, the initial concentration of the adsorbate and concentration at the time, t, respectively, M and V are media mass (g) and wastewater volume (L) respectively. The experiments were conducted in triplicates and then the averages were determined. The results were adapted to the widely used PFO and PSO kinetic equations as described below by Wei et al. [40]. The PFO is described as:

$$\ln\left(q_e - q_t\right) = \ln q_e - k_1 t \qquad (5)$$

For PSO the equation is described as follows:

$$\frac{1}{q_t} = \left(\frac{1}{k_2 q_e^2} + \frac{1}{q_e}\right) \qquad (6)$$

where q_e and q_t (mgg^{-1}) are the adsorption capacities at equilibrium and at any time, t, respectively, k_1 (min^{-1}), k_2 (gmg^{-1} min^{-1}) are the rate constants of PFO and PSO, respectively.

The intraparticle diffusion model as described by Berkessa et al. [41] was used to evaluate whether intraparticle diffusion controls the rates of phosphate and sulphate ions in acid washed copper smelter slag and the equation is:

$$q_t = k_p t^{0.5} \qquad (7)$$

where q_t (mgg^{-1}) is the amount adsorbed at time, t, (min), k_p (mgg^{-1}min$^{1/2}$) is the intraparticle diffusion rate constant.

2.6 Influence of media dosage and equilibrium isotherms

In order to evaluate the effect of the adsorbent dose on PO_4^{3-} P and SO_4^{2-} removal from wastewater, media increments of 0.5 g to 4.0 g were added in triplicate in 250 mL Erlenmeyer flasks, after which 100 mL of wastewater with known PO_4^{3-} P and SO_4^{2-} concentrations were added. One control flask contained only wastewater. Flasks were placed on an orbital shaker and agitated at 120 rpm for 2 h, and the equilibrium time was determined during kinetic studies. The flasks were removed after 2 h, and the mixtures were filtered, PO_4^{3-} P, SO_4^{2-} pH, and temperature were measured as previously described and the averages were determined. The adsorbed amounts of PO_4^{3-} P and SO_4^{2-} were calculated according to the equation proposed by Chung et al. [42]

$$q_e = \frac{(C_0 - C_e)}{M}V \qquad (8)$$

where q_e (mg g^{-1} media), C_o (mg L^{-1}), C_e (mg L^{-1}) are adsorption capacity at equilibrium, initial adsorbate concentration and equilibrium concentration respectively, M and V are adsorbent mass (g) and wastewater volume (L) respectively.

The data were fitted on to the Langmuir and Freundlich adsorption equations for the analyses of the adsorption isotherms as described in [42]. The Langmuir isotherm equation assumes monolayer adsorption process on the surface of the adsorption material and it is calculated as per the equation by Chung et al. [42]:

$$q_{e=\left(\frac{K_L C_e}{1+K_L C_e}\right)q_{max}} \qquad (9)$$

According to the equation, C_e (mg L^{-1}) is the concentration of the adsorbate in the solution, q_e (mg g^{-1} media) is the adsorption capacity of the adsorbent in equilibrium, K_L (Lm g^{-1}) is the Langmuir constant, and qmax (mg g^{-1} media) is related to the maximum adsorption capacity. The linearized Langmuir equation is as per Eq. 7.

$$\frac{1}{q_e} = \left(\frac{1}{K_L q_{max}}\right)\frac{1}{C_e} + \frac{1}{q_{max}} \qquad (10)$$

The dimensionless Langmuir constant, R_L which is the separation factor, provides an idea about the nature of adsorption and was calculated from the equation described by Gupta et al. [43]:

$$R_L = \frac{1}{1 + K_L C_i} \qquad (11)$$

The Freundlich isotherm equation can be represented in the following equation as described by [42].

$$q_e = K_F C_e^{1/n} \qquad (12)$$

The linearized equation as per Karen et al. [44]:

$$ln q_e = ln K_F + \frac{1}{n} ln C_e \qquad (13)$$

where KF (L$^{1/n}$ mg $^{(1-1/n)}$/g) is Freundlich isotherm constant and 1/n is the Freundlich constant, qe (mg g^{-1}) is the adsorption capacity at equilibrium and C_e (mg L^{-1}) is the adsorbate concentration at equilibrium.

2.7 The effect of initial pH

The impact of the pH was investigated by adding 2.5 g of media into different 250 mL Erlenmeyer flasks, and the pH was adjusted by adding 0.1 M HNO$_3$ or 0.1 M NaOH solutions as per [45] protocol. A 100 mL wastewater

having concentrations of 23.95 and 16.73 mg L^{-1} PO$_4^{3-}$ P and SO$_4^{2-}$ respectively was added into the flasks and the pH was adjusted. The flasks were placed onto the orbital shaker and agitated for at 120 rpm for 2 h. The flasks were removed after the specified times, and the mixtures were filtered according to the same protocol as previously described. The PO$_4^{3-}$ P and SO$_4^{2-}$ concentrations in the resulting solutions were measured, and the adsorption capacity was determined from Eq. 2. The experiment was conducted in triplicates, after which the mean and standard deviation were calculated.

2.8 Influence of temperature

The effect of temperature on PO$_4^{3-}$ P and SO$_4^{2-}$ uptake was examined by adding 2.5 g of treated copper smelter slag in triplicate to 250 mL flasks, after which a 100 mL wastewater of PO$_4^{3-}$–P and SO$_4^{2-}$ concentrations of 23.95 mg L^{-1} and 16.73 mg L^{-1}, respectively, was added. The protocol described by Aljeboree et al. [46] was followed. The flasks were placed in a thermo Shaking Incubator, (Thermo Scientific) supplied by Lam World Technologies (PTY) LTD. The mixtures were shaken at a speed of 120 rpm for 120 min at temperatures of 30, 40, 50, and 60 °C. The flasks were then removed from the shaker and the mixtures were filtered through 0.45 μm Whatman papers. The amounts of PO$_4^{3-}$ P and SO$_4^{2-}$ adsorbed at equilibrium were determined and mean values were calculated, and the adsorption capacities were determined as previously described.

2.8.1 Thermodynamics

The linearized thermodynamics equations were used to determine thermodynamic parameters, that were calculated according to the following equations described by Aljeboree et al. [46]. The thermodynamic parameters, Gibbs free energy change (ΔG°), enthalpy (ΔH°) and entropy (ΔS°) were calculated from the equations listed.

Other parameters such as the enthalpy of adsorption (ΔH°), and the entropy (ΔS°) of the adsorption were determined according to Van't Hoff equation [46]:

The change in entropy and enthalpy values were calculated from the slope and intercept of the Van't Hoff's plot.

$$\Delta G^o = -RT\, LnKd \qquad (14)$$

$$LnKo = \frac{-\Delta H}{RT} + \frac{\Delta S}{R} \qquad (15)$$

$$Ko = \frac{Co - Ce}{Ce} x \frac{V}{M} \qquad (16)$$

where ΔG°, ΔS° and ΔH° respectively denote change in Gibbs free energy, entropy and enthalpy in kJ mol^{-1}. The constant Ko denotes the adsorption distribution coefficient, while R (8.314 J/(molK)) and T (K) represent gas constant and absolute temperature, respectively.

2.9 Statistical analysis

The statistical analysis was performed using Microsoft Excel XLSTAT software through which Mean, Standards and Errors were calculated. Some of the relevant data was then analysed through batch kinetic and isotherm models.

3 Results and discussion

3.1 Media characterization

The images of the acid washed copper smelter slag before and after phosphate and sulphates loading are shown in Fig. 1a, b respectively. The slag shows larger cavities and rougher surface compared to previous study conducted by Letina and Letshwenyo [35] in which the adsorbent was smooth. A rough surface suggests the possibility of a better adsorbent. Washing the adsorbent with acid may have removed some dirt and other materials such as residual phosphate therefore opening up of cavities on the slag surfaces. The surface of the adsorbent after adsorption does not show pronounced rougher surface compared to before the adsorption process. The adsorption of phosphate and sulphates ions into micropore could have reduced the rough surface and openings. It is expected that the adsorption process will improve compared to previous results before acid wash. The smoothness of the material after adsorption could be an indication that the adsorption cavities and pores are filled with phosphates

and sulphates molecules [46]. The loaded acid washed copper smelter slag (b) was observed as impregnated and showed some increase in the number of irregular small particles. Gaps could still be observed between the particles, which indicate a loose arrangement [47].

The elemental composition before the acid washing from the previous results [48] and after the acid washing is shown in Table 3, and only those elements which have an affinity for phosphors are shown. The results reveal that calcium, magnesium, and phosphate ions decreased in the acid washed slag, whereas iron, and aluminium had increased concentrations. Calcium is one of the elements that generally precipitate phosphate ions during the process and reducing its concentration could affect phosphate removal. The reduction of residual phosphate ion in the acid washed slag might result in a better phosphorus removal as there are many active sites in the slag for phosphate retention.

The bulk density, particle density and the porosity of the treated copper smelter slag are shown in Table 4 and both are higher than the wastewater density, which could minimise the suspension of the adsorbent during the fixed bed column trials. The bulk density of the adsorbent also gives an indication of the mass of the adsorbent that the

Table 3 XRF results showing elemental composition of the slag before and after acid washing

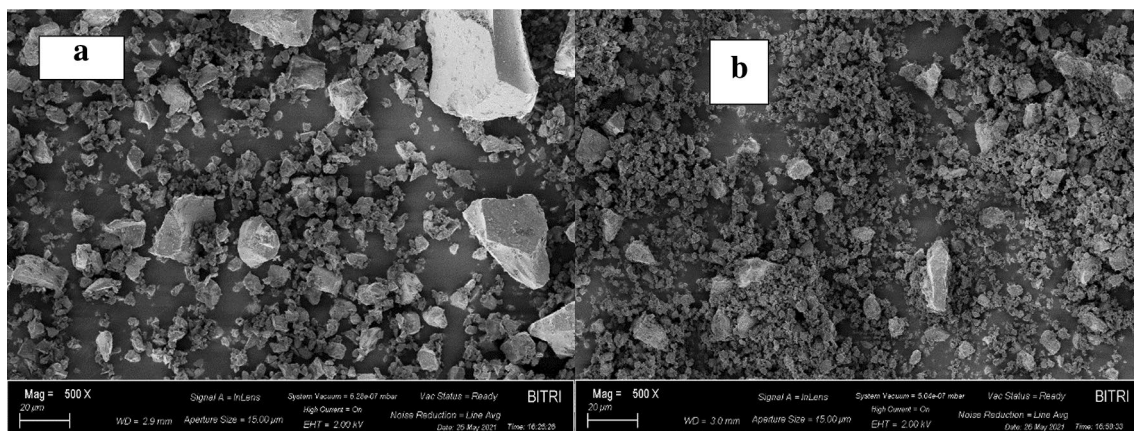| Elemental composition (%)	Before acid washing	After acid washing
Iron	11.2 ± 0.42	27.21 ± 1.92
Calcium	19.82 ± 0.96	1.49 ± 0.15
Magnesium	5.84 ± 0.52	Not detected
Aluminium	1.80 ± 0.28	5.41 ± 0.73
Phosphate	8.79 ± 0.30	0.19 ± 0.003

Fig. 1 Scanning electron microscopy for surface morphology before adsorption (**a**) and after adsorption (**b**)

Table 4 Physical characterisation results of acid washed copper smelter slag

Property	Measured value
Bulk density (g cm^{-3})	1.79 ± 0.01
Particle density (g cm^{-1})	3.45 ± 0.01
Porosity (%)	48.26 ± 0.1

column can accommodate and the liquid weight that the column can retain in as well [49]. The porosity of the adsorbent provides information about the number of pores in the material [49]. The results suggest that a particle had a 48.26% porosity, and this enhances the adsorption process.

Previous studies on the characterisation of untreated copper smelter slag by [32] have shown various mineralogy and chemical contents of the material. The percentage content may have changed as some of the minerals may have reacted with the hydrochloric acid. The morphology of the treated slag may have changed as some of the impurities may have been removed by the acid.

3.2 The point of zero charge

The acid washed copper smelter slag pHpzc is shown in Fig. 2. The pHpzc is at pH 6.04. The previous study by the same author has reported the unwashed copper smelter slag at pH 5.0. The results indicate a positively charged surface of acid washed copper smelter slag at pH < 6.04, and a negatively charged at pH > 6.04. The charge on the surface of the acid washed copper smelter slag at pH 6.04 is zero. When the pH < pHpzc, there might be an increase of hydrogen ion (H$^+$) in the wastewater which will react

with the hydroxyl group on the media surface to form protonated hydroxyl groups [50] and promoting PO$_4$$^{3-}$ P and SO$_4$$^{2-}$ adsorption onto the slag. When the pH > pHpzc, the media surface will have more negative charges and will repel the negatively charged ions (PO$_4$$^{3-}$ P and SO$_4$^{2}). It is anticipated that the adsorption of PO$_4$$^{3-}$ P and SO$_4$$^{2-}$ in the treated copper smelter slag will be dominant at pH values below 6.04. In addition, it is expected that the maximum adsorption capacity will be at pH < pHpzc, and the adsorbent will be electrostatic- positive and the phosphate and sulphate ions are in the anionic forms [50]. In the contrary, when pH > pHpzc, there would be an electrostatic repulsion between media and PO$_4$$^{3-}$ P and SO$_4$$^{2-}$ ions which would lead to a weak bond between the ions and the adsorbent.

3.3 The pH static leachability tests

The leachability of the toxic metals from the acid washed copper smelter slag are shown in Table 5. The results show that all the heavy metals had pH values higher than the national threshold at pH 2, except for Arsenic (As) and Chromium (Cr). However, the pH of wastewater rarely reaches pH 2, so there is less possibility of toxicity effect or secondary pollution from the leaching of metals from the material. The results are similar to the observations made by Ganne et al. [51] who reported leachability of heavy metals from slags at pH 2, but significantly low at other pH values investigated. Furthermore, the findings of this study are similar to those reported by Saha and Sarker [52], who observed low concentrations of heavy metals in concrete using slag as aggregate during the leachability investigation. The results show that the heavy metals leachability from the acid washed copper smelter slag is
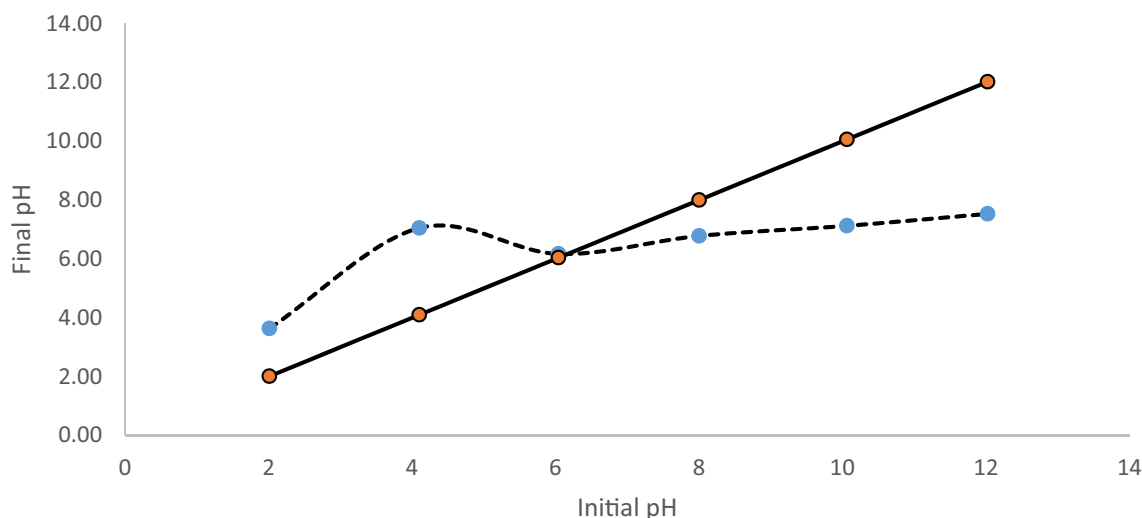

Fig. 2 The point of zero charge for the acid washed copper smelter slag

Table 5 Leachability of heavy metals from treated copper smelter slag at different pH values

pH	Heavy metal concentrations (mg L^{-1})							
	Arsenic	Chromium	Copper	Iron	Manganese	Nickel	Lead	Zinc
2	0.0	0.32	1.8	128.2	0.32	0.67	0.20	0.19
4	0.0	0.0	0.50	0.30	0.00	0.30	0.01	0.04
6	0.0	0.00	0.07	0.02	0.00	0.27	0.01	0.01
8	0.0	0.0	0.02	0.02	0.00	0.18	0.00	0.02
10	0.01	0.00	0.01	0.02	0.00	0.03	0.00	0.01
12	0.00	0.03	0.04	0.08	0.00	0.00	0.01	0.01
Deionised water	0.0	0.02	0.01	0.01	0.00	0.01	0.0	0.02
Botswana Bureau of Standards (BOBS)	0.1	0.5	1.0	2.0	0.1	1.0	0.05	5.0
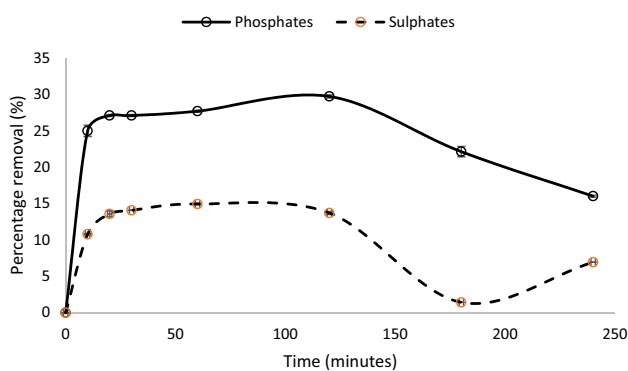
Fig. 3 Effect of contact time on phosphorus and sulphates adsorption onto treated copper smelter slag

minimal, therefore the risk is low when using acid washed copper smelter slag as an adsorbent. The adsorbent can be used with minimal risk of secondary contamination from the material.

3.4 Kinetic modelling

The kinetics study during adsorption is important in determining the rate of adsorption and the mechanisms involved during the process [46]. Figure 3 shows the effect of the contact time on PO_4^{3-} P and SO_4^{2-} adsorption in the treated copper smelter slag. Both graphs are steep in the first 20 min indicating a rapid PO_4^{3-} P and SO_4^{2-} uptake and a gradual decrease thereafter. Equilibrium was reached during the first 20 min in both cases as no percentage or slow removal increases were observed thereafter. The efficiencies for phosphate and sulphate ions removal were 27 and 14% respectively. The percentage removal had decreased by 14% and 8% for SO_4^{2-} and PO_4^{3-} P, respectively, by 180 min suggesting desorption for both ions.

The implications of the results is to minimize the optimal contact time during the process to prevent the

adsorbed adsorbate leaching from the adsorbent and pollution of the environment. Since the adsorbed phosphate can leach from the adsorbent, the saturated slag can be used as soil amendment to enrich the soil for agricultural purposes and improve food security. In addition, desorption might be due to a collision between adsorbent particles and therefore breaking as a result of a high stirring speed. This can be minimised by reducing the agitation speed. Uddin et al. [53] observed an increase in the dye removal as agitation speed was increased, and a decrease in the removal after the equilibrium has been reached. The increase was attributed to the diffusion of dye molecules into the adsorbent pores and to the kinetic energy of the dye molecules [53]. The particle collision started at the highest speed, and the dye molecules were detached [53], and this scenario could apply during our study. Cucarella and Renman [54] have recommended shaking speed between 100 and 200 rpm, although materials can still break at 100 rpm, thereby changing media sizes and porosities and giving higher adsorption capacities.

The adsorption kinetics were further analysed through PFO, PSO and the intraparticle diffusion are presented in Table 5. The plot of PFO is shown in Fig. 4, and it is usually expressed in the first mintes of the kinetic experimnts.

The PSO graph is presented in Fig. 5 and the results are presented in Table 5. The PSO model better fitted the experimental data compared to PFO with R^2 values of both PO_4^{3-} P and SO_4^{2-} adsorption onto smelter slag > 0.99.

The PSO model showed the best fit of the experimental data with R^2 adsorption values of both PO_4^{3-} P and SO_4^{2-} onto the smelter slag > 0.99. The theoretical adsorption capacities for both PO_4^{3-} P and SO_4^{2-} by PSO were similar to the experimental capacities (Table 6). The differences in theoretical and experimental capacities for PO_4^{3-} P were less than 3% and there was no difference in the adsorption capacity for SO_4^2. The results suggest that the process involved chemical reaction which involved valence forces where electrons were shared or exchange between treated smelter slags, hence a chemisorption
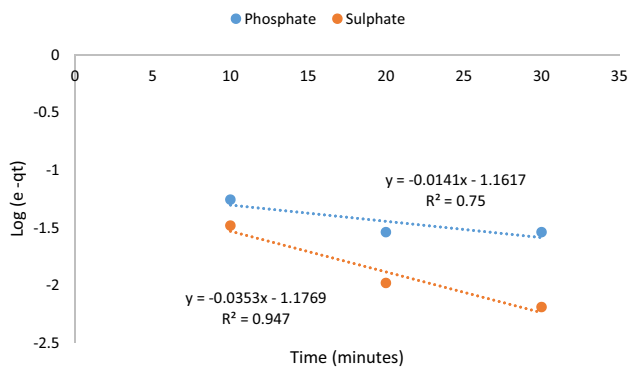
Fig. 4 A pseudo-first order kinetic model of phosphate nd sulphates onto acid washed copper smelter slag
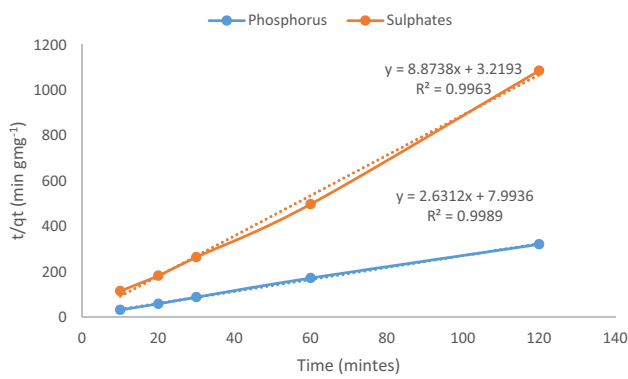

Fig. 5 A pseudo-second order kinetic model of phosphate nd sulphates onto acid washed copper smelter slag

process. Similar results were observed by [39] during the adsorption of phosphorus in phosphorus mine wastes.

Chemisorption through ion-exchange and electrostatic attraction is the most dominant adsorption process by metal (hydr) oxides [50].

The presence of hydroxide (OH^-) groups in metal (hydr) oxides such as iron (Fe), zinc (Zn), and aluminium (Al) promotes the possibility of P–OH ion exchange. These metal oxides were observed in this adsorbent during the previous study by Letshwenyo and Sima [32], hence the possibility of this type of reaction. The bonding could occur through inner sphere complexation by creating covalent chemical bonds between PO_4^{3-} P and metallic cations and the release of other anions [50]. The model assumes that two reactions are occur, the first being fast and reaching equilibrium quickly, followed by the second, slower reaction which lasts longer [55].

The analysis of the kinetic results through the intraparticle diffusion model revealed that there were intercepts (C) of magnitudes of 0.25 and 0.03 mg g^{-1} media for PO_4^{3-} P and SO_4^{2-}, respectively as shown in Fig. 6. For the graphs to reveal intercepts, it shows that the graphs did not pass through the origin, hence intraparticle diffusion was not only controlling the rate of PO_4^{3-} P and SO_4^{2-} adsorption onto smelter slag. In addition to intraparticle diffusion, mechanisms such as film diffusion were also involved in controlling the rate of the adsorption process. The adsorption capacity decreases with decreasing thickness of the boundary layer [56], which suggests that the adsorption of PO_4^{3-} P in the treated copper smelter slag was higher than the adsorption of SO_4^{2}. There were two steps involved during the reactions. The first step was attributed to both the instantaneous adsorption and gradual adsorption, and they were both were involved at the same time, followed by the equilibrium stage where adsorption sites were limited.

Table 6 Kinetic rate constants relating to adsorption of PO_4^{3-} P and SO_4^{2-} onto treated copper. smelter slag

Kinetic parameters	Pseudo first order		Pseudo second order		Intraparticle diffusion	
	Phosphates	Sulphates	Phosphates	Sulphates	Phosphates	Sulphates
K_{ad} (min^{-1})	0.032	0.08				
q_e (mg g^{-1} media)	0.97	1.1	0.38	0.11		
K_p (mg g^{-1} min^0.5)					0.02	0.017
K (g mg^{-1} min^{-1})			0.86	24.6		
H (mg g^{-1} min^{-1})			0.13	0.31		
Qe experimental (mg g^{-1} media)	0.37	0.11	0.37	0.11	0.37	0.11
C (mg g^{-1})					0.25	0.03
R^2	0.75	0.95	0.999	0.996	0.999	0.999

Where K_1, K_2, q_e, K_p, h and C are K_1, K_2 are the rate constants of PFO and PSO respectively, q_e is the adsorption capacities at equilibrium, K_p is the intraparticle rate constant, h is the initial adsorption rate and C is the boundary layer thickness

Fig. 6 Intraparticle diffusion graph of PO_4^{3-} P and SO_4^{2-} adsorption onto acid washed copper smelter slag
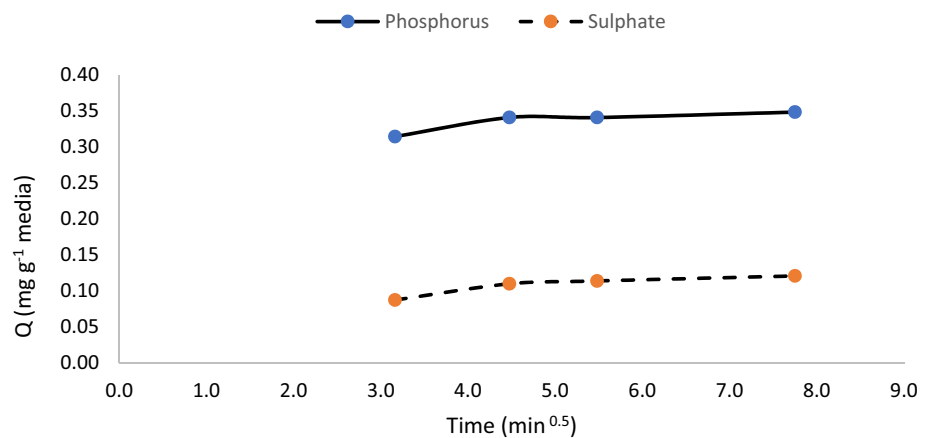
3.5 Effect of media dosage

The adsorption capacities of PO_4^{3-} P and SO_4^{2-} onto smelter slag decreased with the increase in the smelter slag dosage (Fig. 7). The decrease was observed at a media dosage of 3.5 g, and thereafter any increase did not yield any change, suggesting that equilibrium was reached. The uptake of PO_4^{3-} P and SO_4^{2-} decreased with increasing adsorbent dosage because at high adsorbent dosage, the concentrations of PO_4^{3-} P and SO_4^{2-} are not sufficient to occupy all the active sites in the adsorbent resulting in a low uptake of PO_4^{3-} P and SO_4^{2-} [57]. This observation agrees with the findings of this study, in which the adsorption capacities decreased with increasing media dosages. The maximum adsorption capacities were at dosage of 0.5 g/0.1 L of wastewater (5 g L^{-1}) for both PO_4^{3-} P and SO_4^{2-} and this dosage will be the recommended value for practical application. If the concentrations of PO_4^{3-} P and SO_4^{2-} had reduced due to the availability of the adsorption sites as a result of increased media dosage, the available sites would no longer contribute to the removal of the pollutants. A high media dosage can lead to adsorbent

aggregation, thereby reducing the percentage removal of adsorbate [58], which may have been the case in this study. The maximum experimental adsorption capacities of acid washed copper smelter slag for the adsorption of PO_4^{3-} P and SO_4^{2-} were 0.51 and 0.24 mg g^{-1} media, respectively. Washing the adsorbent with the acid may have increased the surface area and the pore volume of the adsorbent, since impurities such as carbonates could have been removed as reported by Santos et al. [12]. The findings of this study are comparable to the observations made by Fathy et al. [59] who reported that the alkali-acid treatment of rice straw enhanced the adsorption capacity of the adsorbent for dye removal. A low dosage of the adsorbent leads to a low usage of the adsorption material, thereby minimizing the quantity required which would last for a long time.

3.5.1 Equilibrium isotherms

Table 7 shows the equilibrium constants from the Freundlich and Langmuir adsorption isotherms plots. The adsorption of both PO_4^{3-} P and SO_4^{2-} in acid washed

Fig. 7 Effect of media dosage on the adsorption of phosphorus and sulphates onto treated copper smelter slag
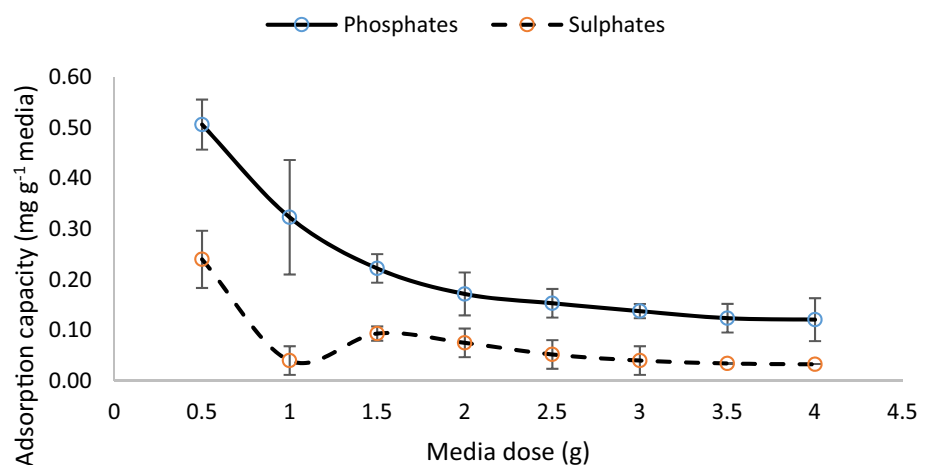
Table 7 Equilibrium isotherm parameters for adsorption of phosphate and sulphate ions onto acid washed copper smelter slag

Equilibrium isotherm	Parameter	Sulphates ion	phosphate ion
Langmuir	Q_{max}	0.08	0.050
	K_L	0.01	0.02
	R^2	0.1	0.90
	R_L	0.86	0.66
Freundlich	K_F	Unrealistic figure	0.00
	n	− 13	12.78
	R^2	0.06	0.84

copper smelter slag was best described by the Langmuir isotherm, as their correlation coefficients were higher than those of the Freundlich isotherm. This suggests that the adsorption process exhibited a monolayer coverage of PO_4^{3-} P and SO_4^{2-} the on the surface of the adsorbent, revealing that the active sites are homogeneous and identical, and no further adsorption of the two anions after the active sites have been covered with the adsorbates [46]. The separation or Langmuir factors (R_L) for the adsorption of the two adsorbates in acid washed copper smelter slag were 0.66 and 0.86 for PO_4^{3-} P and SO_4^{2-}, respectively. Since these values are less than unity (1), this indicates favourable adsorption process [60]. The experimental adsorption capacities for the removal of PO_4^{3-} P and SO_4^{2-} in the adsorbent were 10 and 3 times more than the theoretical values. This shows that adsorption isotherms do not always give realistic results, and pilot scale experiments should be conducted to better understand the process.

3.6 The effect of initial pH

Figure 8 shows the effect of the initial pH on the adsorption capacity of the acid washed copper smelter slag during the removal of PO_4^{3-} P and SO_4^{2-}. The adsorption capacity decreased during the removal of PO_4^{3-} P with increasing pH until pH 4 (0.07 mg PO_4^{3-} P g^{-1} media), and then increased with increasing pH value. The maximum adsorption capacity for the removal of PO_4^{3-} P was observed at pH 12, which was the highest pH observed above pHpzc. At pH > pHpzc, the adsorption of PO_4^{3-} P in acid washed copper smelter slag might be due to the formation of the inner–sphere phosphate adsorption rather than an electrostatic interaction [61]. The results were almost similar to the findings by Liu et al. [62] where it was observed that when the initial pH was increased from 10.0 to 13.0 the removal of PO_4^{3-} P was observed increasing Millero et al. [63] reported that the maximum adsorption capacity of calcite for PO_4^{3-} P was at pH 8.6 and this was associated with the changes in the surface sites of the media or speciation of the phosphate ions in the solution and concluded that this was due to changes in the surfaces of the media. Since calcite mineral was present in the copper smelter slag, this could also have contributed during this study. The SO_4^{2-} may have been competing with PO_4^{3-} P and initially forming $CaSO_4$ as a precursor and then converting to Hydroxyapatite (Hap).

Mustapha et al. [64] reported that the pH is a significant parameter that influences the adsorption process through adsorbent functional groups, surface charges, degree of ionization and solubility of the adsorbent. In contrast, the adsorption capacity of the acid washed copper smelter slag for the removal of SO_4^{2-} was observed to increase with increasing pH, reaching maximum capacity at pH 6 (0.36 mg SO_4^{2-} g^{-1} media) and then decreasing to pH

Fig. 8 Effect of pH on the adsorption of phosphorus and Sulphates onto copper smelter slag
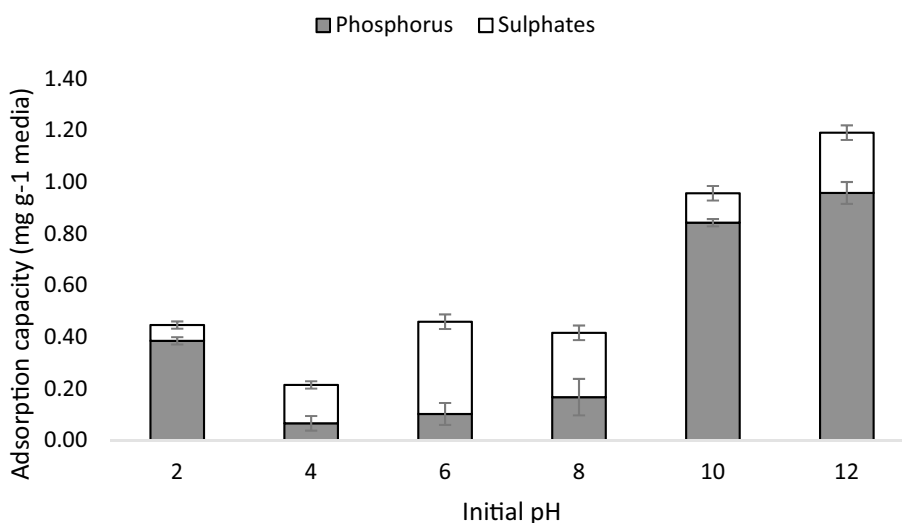
10 and then increasing by 0.12 mg g^{-1} media at pH 12. The results suggest that as the adsorption of the other ion increases, the adsorption of the other ion decreases. Liu et al. [62] observed SO_4^{2-} inhibits the adoption of PO_4^{3-} P at a high concentration, where SO_4^{2-} / PO_4^{3-} P ratios ranged between 6.0 and 15.0 at pH 4.5. It was also reported that lower ratios of 1.5 to 3.0 at pH 4.5 enhanced PO_4^{3-} P removal, and the ratio in this study was 0.7 and it was expected to enhance PO_4^{3-} P removal. The results suggest that PO_4^{3-} P removal was favoured compared to SO_4^{2-}. A better PO_4^{3-} P removal compared to SO_4^{2-} may also be due to an increased solubility of calcite in the presence of $_{SO4}^{2-}$ [62]. The results on the adsorption of SO_4^{2-} differ from the observations reported by Zheng et al. [64] where it was observed that the adsorption capacity of the material decreased with increasing pH. Lower pH values are associated with H^+ ions on the surface of the media, which indicates a high adsorption rate because SO_4^{2-} ions are negatively charged, hence the attraction between media and the SO_4^{2-} ions.

It has been reported by Lin et al. [65] that increasing the pH from 4 to 10 can lead to a decrease in the amount of $H_2PO_4^-$ groups, in which leads to an increase in the HPO_4^{2-} group whose removal is favoured by ligand exchange. This may not have been true for this study as a decrease in pH instead, suggesting that no OH^- ions were released from the media in wastewater, which could increase the pH (Table 4). However, the results indicate a high PO_4^{3-} P adsorption at a high pH above pHpzc. This was also observed by Ye et al. [66] on the adsorption of PO_4^{3-} P on magnesia-pullan. This was attributed to the fact that a high pH only affects the adsorption rate through changing the surface charge of the adsorbent, but the number of OH^- groups is insignificantly influenced, and the same could be true during this study. Liu et al. [67] reported that the dominant PO_4^{3-} P removal mechanism cannot be related to electrostatic attraction just because the removal can still take place at pH > pHpzc.

At pH > pHpzc, the surface of the adsorbent is negatively charged due to the deprotonation of the functional groups of the sorbent which act ion exchangers with PO_4^{3-} P ions, which indicates that the ion exchange was involved in the removal of phosphate by the slag. A high pH during PO_4^{3-} P removal results in the final pH adjustment from 11.49 to 9.5 if the initial pH was 12, and there is no concern if the initial pH is 10 was as it has been observed that the final pH is just within the threshold, and strict monitoring is needed. It has been reported that adsorption occurs on positive, negative or neutral surfaces during specific adsorption when free energy is dominant [68]. The same may have happened during this study as the results revealed higher PO_4^{3-} P retention capacities at pH > pHpzc (pH 10 and 12). For non-specific sorption to be occur, the adsorbent must have an overall positive charge, which is lower than pHpzc during PO43- P and SO42- adsorption, and this was not the case during this study. Therefore, the ion exchange between PO_4^{3-} P, SO_4^{2-} ions and ligands on the slag surface may have been the likely adsorption mechanism [68]. The pH influences the surface properties of the adsorbents and the solution dissociation process of the phosphate and sulphate ions in the solution [44]. For practical purposes of improving the adsorption capacity of the adsorbent, the pH can be altered to a level that promotes retention of the ions by the adsorbent.

3.7 Effect of temperature

Figure 9 shows the effect of temperature on the adsorption of PO_4^{3-} P and SO_4^{2-} in acid-washed copper smelter slag. The results show that there was a slight increase in the adsorption capacity of the media with increasing temperature. The observed increase in adsorption capacity for PO_4^{3-} P and SO_4^{2-} between 30 and 50 °C was 1.4% and 150%, respectively. The maximum increases were observed at 60 °C, which was 39.2% and 188% for PO_4^{3-} P and SO_4^{2-}, respectively. The adsorption capacities at this

Fig. 9 Effect of temperature on PO_4^{3-} P and SO_4^{2-} adsorption by copper smelter slag
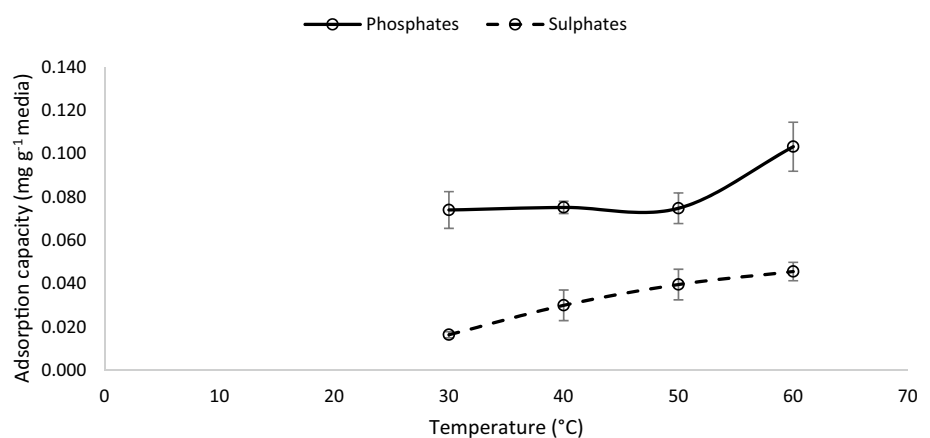
temperature were 0.103 ± 0.09 and 0.046 ± 0.004 mg g^{-1} media for PO_4^{3-} P and SO_4^{2-}, respectively. The adsorption capacities differed to those observed earlier under normal conditions, which were 0.05 mg g^{-1} and 0.15 mg g^{-1} media for SO_4^{2-} and PO_4^{3-} P, respectively. Although the percentage increases are large, the actual increase in adsorption capacity was very small. The same results were reported by Jellali et al. [39] who reported an average rate of increase of 0.07 mg g^{-1} media when the temperature was increased from 20 to 40 °C. This suggests that the process was endothermic due to the increase in the kinetic energy of the acid-washed copper smelter slag particles [39]. High temperatures also promote the rapturing of bonds between functional groups on the slag surface, and thus increase the adsorption sites. The results contradict the observations by Yuan et al. [69] who reported a decrease in PO_4^{3-} P adsorption with increasing temperature, which was an exothermic process. With increasing temperature, the interaction forces between PO_4^{3-} P, SO_4^{2-} and the wastewater weakened when compared to those between PO_4^{3-} P, SO_4^{2-} and the treated copper smelter slag. The PO_4^{3-} P and SO_4^{2-} were then easier to adsorb from wastewater. Since real wastewater was used during the experiment, there might have been other coexisting pollutants such as natural organic matter, humic acid which compete for active sites with PO_4^{3-} P and SO_4^{2-} for adsorption sites leading to low adsorption capacities observed. Since the increase in adsorption was very minimal as temperature was increased, there will not be a need to increase temperature during pilot or field trials. This will reduce the costs of operation and maintenance since there will be no need to raise the temperature of the system.

3.7.1 Thermodynamic studies

The results of the adsorption of the sulphates onto media revealed positive values of ΔG°, ΔH° and ΔS° at all the temperatures investigated (Table 8) and the graphical plot is presented in Fig. 10. In case of phosphate sorption, negative values of ΔG° and ΔS° and positive values of ΔH° were obtained. It has been reported that a positive change in the entropy values indicate a high affinity of the contaminant to the adsorbent and the random solid–liquid interface [70]. This suggest that sulphate ion had high affinity to smelter slag and increased randomness at solid–liquid interface during sorption [70] compared to the limited interaction between phosphate ion and the adsorbent. A spontaneous and non-spontaneous adsorption process is indicated by negative and positive values of change in the Gibbs free energy (ΔG°) [71]. In this case, this reflects that the adsorption of phosphates was a spontaneous process, while the sorption of sulphates was non-spontaneous at all temperature ranges of 303–333 K (Table 7). The adsorption

Table 8 Summary of thermodynamic parameters

Temperature (K)	Pollutant	ΔG° (kJmol^{-1})	ΔH° (kJmol^{-1})	ΔS° (kJmol^{-1})
303	Phosphorus	− 0.00976		
313		− 0.01026	8.9500	− 0.0172
323		− 0.01053		
333		− 0.01545		
303	Sulphate	16.86052		
313		15.77766	0.06761	0.000234
323		15.48571		
333		15.54153		

of both phosphate and sulphate on acid-washed copper smelter slag showed that the process was endothermic, as the ΔH° values were all positive, meaning that energy was required for the sulphate and phosphate ions to migrate to the surface of the media. The results are comparable to the findings reported by Iftekhar et al. [10]. Thermodynamic information such as enthalpy, Gibbs free energy and entropy can provide information about the randomness of the phosphate/sulphate ions at acid-washed copper smelter slag and the wastewater, spontaneity information and heat of adsorption [72].

3.8 Adsorption mechanism

Understanding the nature of adsorption mechanisms, such as physical or chemical reactions between adsorbates and adsorbents helps in knowing the dictating mechanism during the adsorption process. Almanassra et al. [72] reported that the adsorption mechanism is interconnected to processes such as adsorption isotherms, kinetics thermodynamics, and these help in the long-term design of reactors for the water and wastewater treatment. Jellali et al. [39] reported that low significance of other anions (though with high concentrations) during adsorption compared to phosphorus adsorption indicates that inner-sphere complexation is involved. This suggests that adsorption on the surface of the slag had strong chemical bond formations and in agreement with the findings of this study. Since Pseudo-Second Order equation better described kinetic data, it further suggests that chemisorption was dominant during the adsorption process. The adsorption process might be similar to that observed by Yan et al. [73] which was described as phosphorus and sulphates transfer from aqueous solution to adsorption sites followed by chemical complexation or ion exchange at the active sites and lastly precipitation on slag surface (Fig. 11). Phosphate adsorption occurred at higher pH (10 and 12) than at pH < pHpzc when the surface of the

Fig. 10 Van't Hoff's plot for sorption of phosphorus and sulphate onto copper smelter slag at 303,313,323 and 333 K

$y = -8.1318x + 0.0282$
$R^2 = 0.9834$

$y = -1076.5x - 2.0654$
$R^2 = 0.601$

Ln K_d

$1/T(K^{-1})$
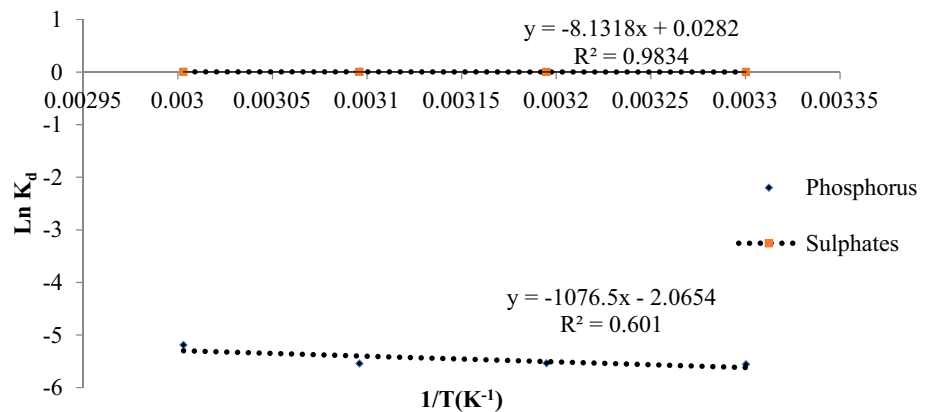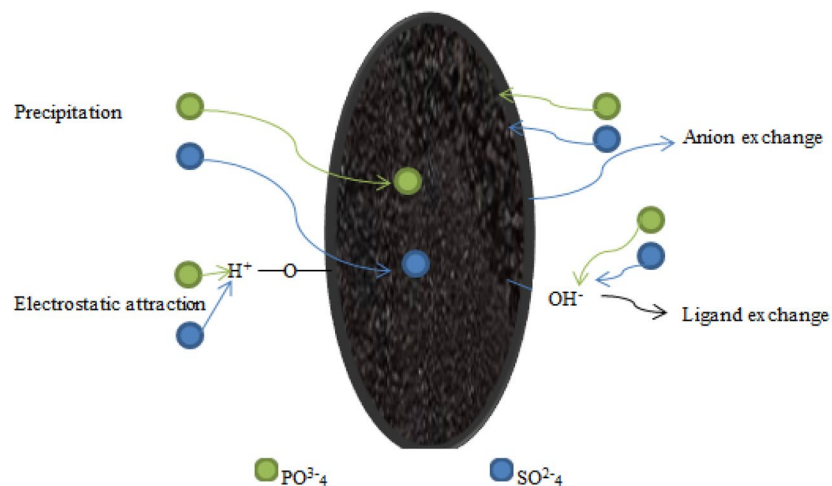
Phosphorus

Sulphates

Fig. 11 Schematic diagram of adsorption mechanism by acid washed copper smelter slag

slag was supposed to have a negative charge similar to phosphates and sulphates ions. This may have been due to a specific adsorption, since adsorption occurs on positive, negative and neutral surfaces as observed by Almasri et al. [68]. The increase in the adsorption capacity with increasing temperature suggests that the process was endothermic. Another observation through intraparticle diffusion results suggests that intraparticle diffusion and other mechanisms such as film or external diffusion were involved in the adsorption process.

3.9 Practical implications

The success of this study will benefit the country and the environment by reducing the costs associated with disposal of slag wastes. It will reduce pollution effects caused by phosphate and sulphate discharges. The low adsorption efficacy observed in this study requires further investigation into other possible uses of the copper smelter slag rather. The conventional wastewater treatment methods are known for their high energy requirements, high carbon footprints and large quantities of unusable toxic sludge [74]. The success of the

study will reduce the costs of sludge disposal and its toxicity effects on the environment [75]. There is a need to conduct another study on the same adsorbent at a pilot scale through fixed bed columns. During the current study, the adsorbent particle sizes ranged from 1.18 to 4.36 mm, which may have contributed to a low adsorption capacity and is unlike other studies where smaller particle sizes are used. The effect of the particle size could be investigated in the future to determine the appropriate size that leads to a higher adsorption capacity. In addition, the agitation speed was not investigated, the study was conducted at only 120 rpm and additional studies at different shaking speeds could yield better results. Conducting the study in the fixed bed column mode could have improved the efficiency of the adsorbent because the depth of the column can be changed to find a suitable bed depth. The copper smelter slag should be disposed of in an environmentally friendly manner. There is an ongoing research in the same department investigating copper smelter slag as aggregate for brick moulding. This is an ideal way to dispose the slag without polluting the environment. It will also reduce the costs of disposing the saturated adsorbents.

Another disposal option is to use the spent adsorbent as cover material on a local landfill and as aggregate for road maintenance. Such activities will reduce the possibilities of environmental pollution resulting from the saturated adsorbents.

4 Conclusion

This study investigated acid-washed copper smelter slag for the removal of phosphorus and sulphates from wastewater. There was no secondary pollution released from the adsorbent as no heavy metals were released. Desorption of phosphates and sulphates was observed when the contact time was increased and this may be observed during pilot scale or field application. The treated slag showed improved the adsorption capacity for phosphorus to 0.51 mg PO_4^{3-} P g^{-1} media from previous results of 0.26 mg PO_4^{3-} P g^{-1} media, and the capacity was observed decreasing with increasing media dosage as a result of many available active sites on the adsorbent and low concentration of ions in the solution. The acid-washed copper smelter slag adsorption capacity for sulphate adsorption was 0.24 mg SO_4^{2-} g^{-1} media. The highest adsorption capacity of phosphorus was 0.96 mg PO_4^{3-} P g^{-1} media observed at pH 12, and SO_4^{2-} was 03.9 mg SO_4^{2-} g^{-1} media observed at pH 2. Temperature had no significant effect during the adsorption process and the thermodynamic studies suggested and endothermic process. Although there was an improved adsorption capacity of the acid-washed slag, it would be expensive for practical use in slag treatment. For practical purposes, it will be necessary to adjust the pH before discharge into the environment if the wastewater pH was to be adjusted to remove either PO_4^{3-} P or sulphates. Overall, the study showed that a high pH could enhance PO_4^{3-} P adsorption by the treated copper smelter slag. It may not be necessary to treat the slag as pH adjustment would enhance the removal capacity of the adsorbent. Other modifications to enhance performance, such as heat treatment should be explored.

Data availability Data is available upon request.

Declarations

Conflict of interest The authors have no conflicts of interest to declare that are relevant to the content of this article.

References

1. Copetti D, Finsterle K, Marziali L et al (2016) Eutrophication management in surface waters using lanthanum modified bentonite: a review. Water Res 97:162–174. https://doi.org/10.1016/j.watres.2015.11.056
2. Khan MA, Wen J (2021) Evaluation of physicochemical and heavy metals characteristics in surface water under anthropogenic activities using multivariate statistical methods, Garra River, Ganges Basin, India. Environ Eng Res 26(6):1
3. Huang W, Wang S, Zhu Z et al (2008) Phosphate removal from wastewater using red mud. J Hazard Mater 158:35–42. https://doi.org/10.1016/j.jhazmat.2008.01.061
4. Bunce JT, Ndam E, Ofiteru ID, Moore A, Graham DW, Graham DW (2018) A review of phosphorus removal technologies and their applicability to small-scale domestic wastewater treatment systems. Front Environ Sci 6:1–15. https://doi.org/10.3389/fenvs.2018.00008
5. Chai C, Zhang D, Yu Y, Feng Y, Wong MS (2015) Carbon footprint analyses of mainstream wastewater treatment technologies under different sludge treatment scenarios in China. Water 7:918–938. https://doi.org/10.3390/w7030918
6. Campos JL, Pedrouso A, Río AV, Belmonte M (2016) Greenhouse Gases emissions from wastewater treatment plants: minimization, treatment, and prevention. J Chem. https://doi.org/10.1155/2016/3796352
7. Renu MA, Singh K (2017) Heavy metal removal from wastewater using various adsorbents: a review. J Water Reuse Desal 7:387–419
8. Suresh P, Korving L, Van Loosdrecht MCM (2019) Adsorption as a technology to achieve ultra-low concentrations of phosphate: research gaps and economic analysis. Water Res X 4:100029
9. Crini G, Lichtfouse E (2020) Advantages and disadvantages of techniques used for wastewater treatment. Environ Chem Lett 17(1):145–155
10. Iftekhar S, Emin M, Srivastava V, Repo E (2018) Application of zinc-aluminium layered double hydroxides for adsorptive removal of phosphate and sulfate: equilibrium, kinetic and thermodynamic. Chemosphere 209:470–479
11. Fang P, Tang Z, Chen X, Huang J, Tang Z, Cen C (2018) Removal of high-concentration sulfate ions from the sodium alkali FGD wastewater using ettringite precipitation method: factor assessment, feasibility, and prospect. J Chem. https://doi.org/10.1155/2018/1265168
12. Santos JDL, Cornejo-bravo JMC, Bogdanchikova EN, Farías SM (2015) Elimination of sulfates from wastewaters by natural aluminosilicate modified with uric acid. Resour Technol 1(2):98–105
13. Zou Y, Zhang R, Wang L, Xue K, Chen J (2020) Applied Clay Science Strong adsorption of phosphate from aqueous solution by zirconium-loaded. Appl Clay Sci 192(January):105638. https://doi.org/10.1016/j.clay.2020.105638

14. Ngatia LW, Hsieh PY, Nemours D, Fu R, Taylor RW (2017) Potential phosphorus eutrophication mitigation strategy: biochar carbon composition, thermal stability and pH in fl uence phosphorus sorption. Chemosphere 180:201–211

15. Wang C, Bai L, Pei Y (2013) Assessing the stability of phosphorus in lake sediments amended with water treatment residuals. J Environ Manage 122:31–36. https://doi.org/10.1016/j.jenvman.2013.03.007

16. Razali M, Zhao YQ, Bruen M (2007) Effectiveness of a drinking-water treatment sludge in removing different phosphorus species from aqueous solution. Sep Purif Technol 55:300–306. https://doi.org/10.1016/j.seppur.2006.12.004

17. Hur J, Shin J, Yoo J, Seo YS (2015) Competitive adsorption of metals onto magnetic graphene oxide: comparison with other carbonaceous adsorbents. Sci World J. https://doi.org/10.1155/2015/836287

18. Xie J, Lin Y, Li C, Wu D, Kong H (2015) Removal and recovery of phosphate from water by activated aluminum oxide and lanthanum oxide. Powder Technol 269:351–357. https://doi.org/10.1016/j.powtec.2014.09.024

19. Wang S, Kong L, Long J et al (2018) Adsorption of phosphorus by calcium-flour biochar: Isotherm, kinetic and transformation studies. Chemosphere 195:666–672. https://doi.org/10.1016/j.chemosphere.2017.12.101

20. Zhou R, Wang Y, Zhang M (2019) Adsorptive removal of phosphate from aqueous solutions by thermally modified copper tailings. Environ Monit Assess 191(198):2019. https://doi.org/10.1007/s10661-019-7336-0

21. Choi JW, Lee SY, Lee SH et al (2012) Comparison of surface-modified adsorbents for phosphate removal in water. Water Air Soil Pollut 223(6):2881–2890. https://doi.org/10.1007/s11270-011-1072-6

22. Ding S, Fang D, Pang Z et al (2018) Immobilization of powdery calcium silicate hydrate via PVA covalent cross-linking process for phosphorus removal. Sci Total Environ 645:937–945. https://doi.org/10.1016/j.scitotenv.2018.07.197

23. Dong R, Liu Y, Wang X, Huang J (2011) Adsorption of sulfate ions from aqueous solution by surfactant modified palygorskite. J Chem Eng Data 56:3890–3896

24. Li J, Wu B, Zhou T, Chai X (2018) Preferential removal of phosphorus using modified steel slag and cement combination for its implications in engineering applications. Environ Technol Innov 10:264–274

25. Solgi M, Tabil GL, Wilson DL (2020) Modified biopolymer adsorbents for column treatment of sulfate species in saline aquifers. Materials 13(2408):2020. https://doi.org/10.3390/ma13102408

26. Alimohammadi V, Sedighi M, Jabbari E (2017) Optimization of sulfate removal from wastewater using magnetic multi-walled carbon nanotubes by response surface methodology. Water Sci Technol 6(10):2593–2602

27. Runtti H, Tuomikoski S, Kangas T, Kuokkanen T, Rämö J (2016) Sulphate removal from water by carbon residue from biomass gasification: effect of chemical modification methods on sulphate removal efficiency. BioResources 11:3136–3152

28. Wei C, Hai-cheng L (2014) Adsorption of sulfate in aqueous solutions by organo-nano-clay: adsorption equilibrium and kinetic studies. J Cent South Univ. https://doi.org/10.1007/s11771-014-2145-7

29. Sadik R, Lahkale R, Hssaine N, Elhatimi W, Diouri M, Sabbar E (2015) Sulfate removal from wastewater by mixed oxide-LDH: equilibrium, kinetic and thermodynamic studies. J Mater Environ Sci 6(10):2895–2905

30. Dong C, Wu X, Gao Z, Yang P, Yawar M, Khan AA (2021) Novel and efficient metal oxide fluoride absorbent for drinking water safety and sustainable development. Sustainabilty. https://doi.org/10.3390/su13020883

31. Khatri N, Tyagi S (2015) Frontiers in Life Science Influences of natural and anthropogenic factors on surface and groundwater quality in rural and urban areas. Front Life Sci 8(1):23–39. https://doi.org/10.1080/21553769.2014.933716

32. Letshwenyo MW, Sima TV (2020) Phosphorus removal from secondary wastewater effluent using copper smelter slag. Heliyon 6:e04134

33. Gu S, Qian Y, Jiao Y, Li Q, Pinay G, Gruau G (2016) An innovative approach for sequential extraction of phosphorus in sediments: ferrous iron P as an independent P fraction". Water Res 103:352–361

34. Dan-Asabe B, Yaro SA, Yawas DS, Aku SY (2013) Water displacement and bulk densityrelation methods of finding density of powdered materials. Int J Innov Res Sci Eng Technol 2(9):6

35. Letina D, Letshwenyo MW (2018) Investigating waste rock, tailings, slag and coal ash clinker as adsorbents for heavy metals: batch and column studies. Phys Chem Earth 105:184–190

36. Letshwenyo MW, Mokgosi S (2021) Investigation of water treatment sludge from drinking water treated with Zetafloc 553I coagulant for phosphorus removal from wastewater. J Environ Manage 282:111909

37. Faria PCC, Órfão JJM, Pereira FRM (2004) Adsorption of anionic and cationic dyes on activated carbons with different surface chemistries. Water Res 38(8):2043–2052

38. Król A, Mizerna K, Bo M (2019) An assessment of pH-dependent release and mobility of heavy metals from metallurgical slag. J Hazard Mater 384:2020

39. Jellali S, Wahab MA, Hassine RB, Hamzaoui AH, Bousselmi L (2011) Adsorption characteristics of phosphorus from aqueous solutions onto phosphate mine wastes. Chem Eng J 169(1–3):157–165. https://doi.org/10.1016/j.cej.2011.02.076

40. Wei J, Xu J, Mei Y, Tan Q (2019) Applied Clay Science Chloride adsorption on aminobenzoate intercalated layered double hydroxides: kinetic, thermodynamic and equilibrium studies. Appl Clay Sci 2020(187):105495. https://doi.org/10.1016/j.clay.2020.105495

41. Berkessa YW, Mereta ST, Feyisa FF (2019) Simultaneous removal of nitrate and phosphate from wastewater using solid waste from factory. Appl Water Sci 9:28

42. Chung H, Kim W, Park J, Cho J, Jeong T, Park P (2015) Application of Langmuir and Freundlich isotherms to predict adsorbate removal efficiency or required amount of adsorbent. J Ind Eng Chem 28:241–246

43. Gupta S, Sharma SK, Kumar A (2019) Biosorption of Ni(II) ions from aqueous solution using modified Aloe barbadensis Miller leaf powder. Water Sci Eng 12(1):27–36

44. Karen A, Estrada C, Lozano FC, Alejandro R, Díaz L (2021) Thermodynamics and kinetic studies for the adsorption process of methyl orange by magnetic activated carbons. Air Soil Water 14:1–11

45. Padmavathy KS, Madhu G, Haseena PV (2016) A study on effects of pH, adsorbent dosage, time, initial concentration and adsorption isotherm study for the removal of hexavalent chromium (Cr(VI)) from wastewater by magnetite nanoparticles. Procedia Technol 24:585–594

46. Aljeboree AM, Alshirifi AN, Alkaim AF (2017) Kinetics and equilibrium study for the adsorption of textile dyes on coconut shell activated carbon. Arab J Chem 10:S3381–S3393

47. Fan B, Jia L, Wang Y, Zhao R, Mei XS, Liu YY, Jin Y (2018) Study on adsorption mechanism and failure characteristics of CO_2 adsorption by potassium-based adsorbents with different supports. Materials 11:2424

48. Sima TV, Letshwenyo MW, Lebogang L (2018) Efficiency of waste clinker ash and iron oxide tailings for phosphorus removal from tertiary wastewater: batch studies. Environ Technol Innov 11:49–63

49. Ekpete OA, Harcourt P (2014) Preparation and characterization of activated carbon derived from fluted pumpkin stem waste (Telfairia occidentalis Hook F). Res J Chem Sci 1:10–17

50. Li M, Liu J, Xu Y, Qian G (2016) Phosphate adsorption on metal oxides and metal hydroxides: a comparative review. Environ Rev. https://doi.org/10.1139/er-2015-0080

51. Ganne P, Buve L, Swennen R (2006) Leachability of heavy metals and arsenic from slags of metal extraction industry at Angleur (eastern Belgium). Sci Total Environ 356:69–85. https://doi.org/10.1016/j.scitotenv.2005.03.022

52. Saha AK, Sarker PK (2017) Sustainable use of ferronickel slag fine aggregate and fly ash in structural concrete: mechanical properties and leaching study. J Clean Prod 162:438–448. https://doi.org/10.1016/j.jclepro.2017.06.035

53. Uddin MK, Nasar A (2020) Walnut shell powder as a low- cost adsorbent for methylene blue dye: isotherm, kinetics, thermodynamic, desorption and response surface methodology examinations. Sci Rep 10:1–13

54. Cucarella V, Renman G (2009) Phosphorus sorption capacity of filter materials used for on-site wastewater treatment determined in batch experiments: a comparative study. J Environ Qual. https://doi.org/10.2134/jeq2008.0192

55. Rosa A, Cristiani-urbina MC, Cristiani E (2015) Chromium biosorption from Cr (VI) aqueous solutions by cupressus lusitanica bark: kinetics, Equilibrium and Thermodynamic Studies. PLoS ONE. https://doi.org/10.1371/journal.pone.0137086

56. Bouamra F, Drouiche N, Abdi N, Grib H, Mameri N, Lounici H (2018) Removal of phosphate from wastewater by adsorption on marble waste: effect of process parameters and kinetic modeling national and international water standard authorities with. Int J Environ Res 12(1):13–27. https://doi.org/10.1007/s41742-018-0065-3

57. Balasubramanian R, Perumal SV, Vijayaraghavan K (2009) Equilibrium isotherm studies for the multicomponent adsorption of lead, zinc and cadmium onto Indonesian peat. Ind Eng Chem Res 48(4):2093–2099. https://doi.org/10.1021/ie801022p

58. Zhou Y, Nie H, Branford-white C, He Z, Zhu L (2009) Removal of Cu 2 + from aqueous solution by chitosan-coated magnetic nanoparticles modified with α -ketoglutaric acid. J Colloid Interface Sci 330(1):29–37. https://doi.org/10.1016/j.jcis.2008.10.026

59. Fathy NA, El-shafey OI, Khalil LB (2013) Effectiveness of alkali-acid treatment in enhancement the adsorption capacity for rice straw: the removal of methylene blue dye. ISRN Phys Chem. https://doi.org/10.1155/2013/208087

60. Ayawei N, Ebelegi AN, Wankasi D (2017) Modelling and interpretation of adsorption isotherms. J Chem. https://doi.org/10.1155/2017/3039817

61. Su Y, Cui H, Li Q, Gao S, Shang JK (2013) Strong adsorption of phosphate by amorphous zirconium oxide nanoparticles. Water Res 47(14):5018–5026

62. Liu Y, Sheng X, Dong Y, Ma Y (2019) Removal of high-concentration phosphate by calcite: effect of sulfate and pH. Desalination 289:66–71

63. Millero F, Huang F, Zhu X, Liu X, Zhang J (2001) Adsorption and desorption of phosphate on calcite and aragonite in seawater. J Chem. https://doi.org/10.1155/2017/3039817

64. Mustapha S, Ndamitso DTSMM, Sumaila MBEA (2019) Adsorption isotherm, kinetic and thermodynamic studies for the removal of Pb (II), Cd (II), Zn (II) and Cu (II) ions from aqueous solutions using Albizia lebbeck pods. Appl Water Sci 9(6):1–11

65. Lin J, Wang X, Zhan Y (2018) Effect of precipitation pH and coexisting magnesium ion on phosphate adsorption onto hydrous zirconium oxide. J Environ Sci 76:167–187

66. Ye Y, Jiao J, Kang D, Jiang W, Kang J, Ngo HH, Guo W, Liu Y (2019) The adsorption of phosphate using a magnesia: pullulan composite: kinetics, equilibrium, and column tests. Environ Sci Pollut. https://doi.org/10.1007/s11356-019-04858-z

67. Liu R, Chi L, Wang X, Sui Y, Wang Y, Arandiyan H (2018) Review of metal (hydr) oxide and other adsorptive materials for phosphate removal from water. J Environ Chem Eng 6(4):5269–5286

68. Almasri DA, Saleh NB, Atieh MA, Mckay G, Ahzi S (2019) Adsorption of phosphate on iron oxide doped halloysite nanotubes. Sci Rep 9(3232):1–13. https://doi.org/10.1038/s41598-019-39035-2

69. Yuan X, Xia W, An J, Yin J, Zhou X, Yang W (2015) Kinetic and thermodynamic studies on the phosphate adsorption removal by dolomite mineral. J Chem. https://doi.org/10.1155/2015/853105

70. Bouhamed F, Elouear Z, Bouzid J (2012) Adsorptive removal of copper(II) from aqueous solutions on activated carbon prepared from Tunisian date stones: equilibrium, kinetics and thermodynamics. J Taiwan Inst Chem Eng 43(5):741–749

71. Mahdavi S, Hassani A, Merrikhpour H (2020) Aqueous phosphorous adsorption onto SnO2 and WO3 nanoparticles in batch mode: kinetic, isotherm and thermodynamic study. J Exp Nanosci 15(1):242–265

72. Almanassra WI, Mckay G, Kochkodan V, Ali M, Al-Ansari T (2021) A state of the art review on phosphate removal from water by biochars. Chem Eng J 409:128211

73. Yan L, Xu Y, Yu H, Xin X, Wei Q, Du B (2010) Adsorption of phosphate from aqueous solution by hydroxy-aluminum, hydroxy-iron and hydroxy-iron: aluminum pillared bentonites. J Hazard Mater 179(1–3):244–250

74. Younas F, Mustafa A, Farooqi R et al (2021) Current and emerging adsorbent technologies for wastewater treatment: trends, limitations, and environmental implications. Water 1:1–25. https://doi.org/10.3390/w13020215

75. Bogusz A, Oleszczuk P, Dobrowolski R (2019) Adsorption and desorption of heavy metals by the sewage sludge and biochar-amended soil. Environ Geochem Health 41(4):1663–1674